

Plague Phylodynamics and Phylogeography

This manuscript ([permalink](#)) was automatically generated from [ktmeaton/obsidian-public@f01a5b57](#) on May 21, 2021.

Authors

- **Katherine Eaton**

 [0000-0001-6862-7756](#) ·  [ktmeaton](#)

McMaster Ancient DNA Center; Department of Anthropology, McMaster University

- **Leo Featherstone**

 [0000-0002-8878-1758](#)

The Peter Doherty Institute For Infection and Immunity , University of Melbourne

- **Sebastian Duchene**

 [0000-0002-2863-0907](#) ·  [sebastianduchene](#)

The Peter Doherty Institute For Infection and Immunity , University of Melbourne

- **Hendrik Poinar**

 [0000-0002-0314-4160](#)

McMaster Ancient DNA Center; Department of Anthropology, McMaster University

Keywords

- Plague
- Yersinia pestis
- Phylodynamics
- Phylogeography

Introduction

Plague has an impressively long and expansive history as a human pathogen. The earliest evidence of the plague bacterium *Yersinia pestis* comes from ancient DNA studies, dating its emergence to at least the Neolithic [1,2]. Since then, *Y. pestis* has traveled extensively due to ever-expanding global trade networks and the ability to infect a diverse array of mammalian hosts [3,4]. Few regions of the ancient and modern world remain untouched by this disease, as plague has an established presence on every continent except Oceania [5].

Accompanying this prolific global presence is unnervingly high mortality. The infamous medieval Black Death is estimated to have killed more than half of Europe's population [6]. This virulence can still be observed in the post-antibiotic era, where case fatality rates range from 22-71% [7]. As a result, plague maintains its status as a disease that is of vital importance to current public health initiatives.

This high priority disease status is unsurprising given that *Y. pestis* is a member of the Enterobacteriaceae family. This family includes enteric pathogens such as *Escherichia coli* and *Salmonella typhi* that are commonly transmitted by contaminated food and water. In comparison, the plague bacterium is unique among this family due to a striking difference in host habitat and transmission. *Y. pestis* commonly resides in the blood of its mammalian hosts and can be transmitted to new hosts through an infectious fleabite [8]. In addition to these tissues, the plague bacterium is also capable of colonizing parts of the mammalian immune system including the lymphatic and reticuloendothelial systems. The large diversity of media in which *Y. pestis* has adapted to colonize is particularly surprising given that it only recently (within the last 20,000 years) diverged as a clone of its parent species *Yersinia pseudotuberculosis* [9].

Despite a close genetic similarity between *Y. pestis* and *Y. pseudotuberculosis*, in which they share 97% gene identity, they differ widely in their transmission and pathogenicity [10]. Whereas *Y. pseudotuberculosis* causes gastrointestinal disease and is transmitted by the food-borne route, *Y. pestis* is primarily transmitted between mammalian hosts by fleas and causes septicemia, pneumonia, and lymphadenitis. Because of this apparent contradiction of genetic homogeneity and diverse phenotypes, an extensive body of research has formed to address how, when, and where, these epidemiological shifts occurred.

TO BE DONE:

- Introduce the topics phylodynamics and phylogeography and what is known so far.
- Introduce the major problem(s) and our objective(s).

Objectives

1. Curate and critique publicly available *Y. pestis* genomes. Discuss how sampling bias drives our current understanding of plague.
2. To propose a nuanced phylodynamics model.
3. To critique interpretations drawn from phylogeographic approaches?

Materials and Methods

Workflow Overview

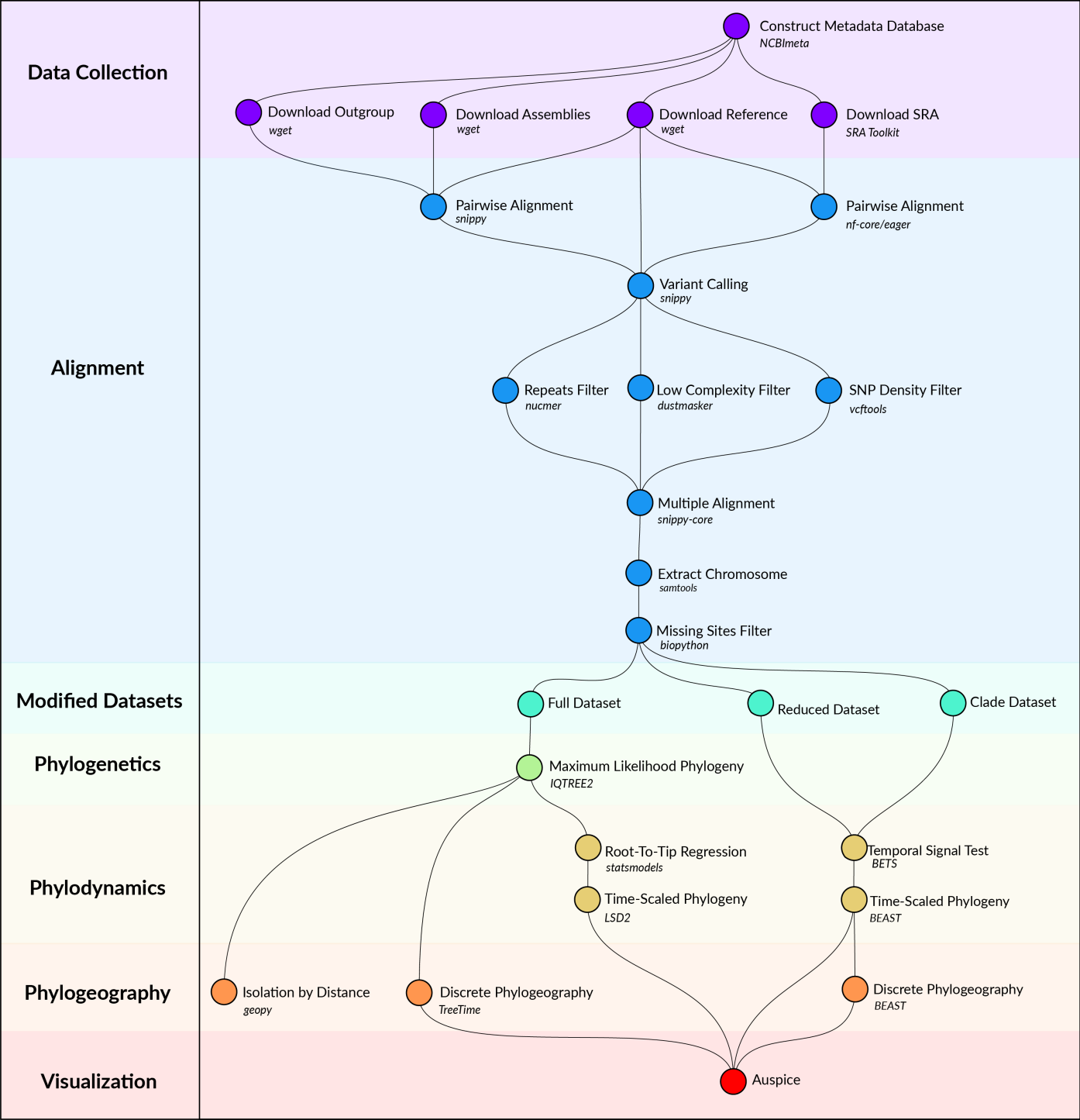


Figure 1: Computational methods workflow.

Data Collection

Y. pestis genome sequencing projects were retrieved from the NCBI databases using NCBImeta [11]. 1657 projects were identified and comprised three genomic types:

- 586 modern assembled
- 184 ancient unassembled
- 887 modern unassembled

The 887 modern unassembled genomes were excluded from this project, as the wide variety of laboratory methods and sequencing strategies precluded a standardized workflow. In contrast, the 184 ancient unassembled genomes were retained given the relatively standardized, albeit specialized, laboratory procedures required to process ancient tissues. Future work will investigate computationally efficient methods for integrating more diverse datasets.

Collection location, collection date, and collection host metadata were curated by cross-referencing the original publications. Collection location was transformed to latitude and longitude coordinates using GeoPy and the Nominatim API for OpenStreetMap [12,13,14]. Coordinates were standardized at a sub-country resolution, taking the centroid of the parent province/state. Collection dates were standardized according to their year, and recording uncertainty arising from missing data and radiocarbon estimates. Collection host was the most diverse field with regards to precision, ranging from colloquial nomenclature (“rat”) to a genus species taxonomy (“*Meriones libycus*”). For the purposes of this study, collection host was recorded as *Human*, *Non-Human*, or *Not Available*, given the inability to differentiate non-human mammalian hosts.

Genomes were removed if no associated date or location information could be identified in the literature, or if there was documented evidence of laboratory manipulation.

Two additional datasets were required for downstream analyses. First, *Y. pestis* strain CO92 (GCA_000009065.1) was used as the reference genome for sequence alignment and annotation. Second, *Yersinia pseudotuberculosis* strains NCTC10275 (GCA_900637475.1) and IP32953 (GCA_000834295.1) served as an outgroup to root the maximum likelihood phylogeny.

Alignment

Modern assembled genomes were aligned to the reference genome using Snippy, a pipeline for core genome alignments [15]. Modern genomes were removed if the number of sites covered at a minimum depth of 10X was less than 70% of the reference genome.

Ancient unassembled genomes were downloaded from the SRA database in FASTQ format using the SRA Toolkit [16]. Pre-processing and alignment to the reference genome was performed using the nf-core/eager pipeline, a reproducible workflow for ancient genome reconstruction [17]. Ancient genomes were removed if the number of sites covered at a minimum depth of 3X was less than 70% of the reference genome. It is a typical approach to relaxed coverage thresholds for ancient genomes relative to modern genomes (CITE). This threshold is commonly used, and aims to strike a balance between variant confidence and sample representation (CITE).

A multiple sequence alignment was constructed using the Snippy Core module of the Snippy pipeline. The output alignment was filtered to only include chromosomal variants and to exclude sites that had more than 5% missing data.

Modified Datasets

To investigate the influence of between-clade variation in substitution rates, the multiple alignment was separated into the major clades of *Y. pestis*, which will be referred to as the *Clade* dataset. Clade and subclade labeling was derived from the five-branch population structure accompanied by a biovar abbreviation ([18]). Only one modification was made, in that the subclade associated with the Plague of Justinian (0.ANT4) was considered to be a distinct clade from its parent (0.ANT) due to its geographic, temporal, and ecological uniqueness. In total, 12 clades were considered and are described in Table 1.

To improve the performance and convergence of Bayesian analysis, a subsampled dataset was constructed and will be referred to as the *Reduced* dataset. Clades that contained multiple samples drawn from the same geographic location and the same time period were reduced to one representative sample. The sample with the shortest terminal branch length was prioritized, to diminish the influence of uniquely derived mutations on the estimated substitution rate. An interval of 25 years was identified as striking an optimal balance, resulting in 200 representative samples.

Phylogenetics

Model selection was performed using Modelfinder which identified the K3Pu+F+I model as the optimal choice based on the Bayesian Information Criterion (BIC) [19]. A maximum-likelihood phylogeny was then estimated across 10 independent runs of IQTREE [20]. Branch support was evaluated using 1000 iterations of the ultrafast bootstrap approximation, with a threshold of 95% required for strong support [21].

Phylogenetics

Temporal Signal

To explore the degree of temporal signal present in the data, two categories of tests were performed. The first was a root-to-tip (RTT) regression on collection date. This linear model is a simple approach to explore whether the data follows a strict clock model. Uncertainty in the model parameters, namely the mean substitution rate and tMRCA, were estimated using 1000 iterations of the non-parametric bootstrap on the residuals.

While RTT is a practical approach, it has two main limitations: 1) No rate variation is accounted for, and 2) The data are not independent observations due to shared internal branch lengths. Therefore to complement this approach, a bayesian evaluation of temporal signal (BETS) was performed.

Rate Variation

A bayesian timetree was estimated using ... as implemented in BEAST.

Time Tree

A maximum-likelihood timetree was estimated using a least-squares approach as implemented in LSD2 [22]. Rate variation was modeled using a lognormal relaxed clock with default parameters for the mean (1.0) and the standard deviation (0.2). The outgroup *Y. pseudotuberculosis* was used to root the tree and then subsequently removed.

Note: I'm still pondering the best choice of parameters for the LSD2 relaxed clock.

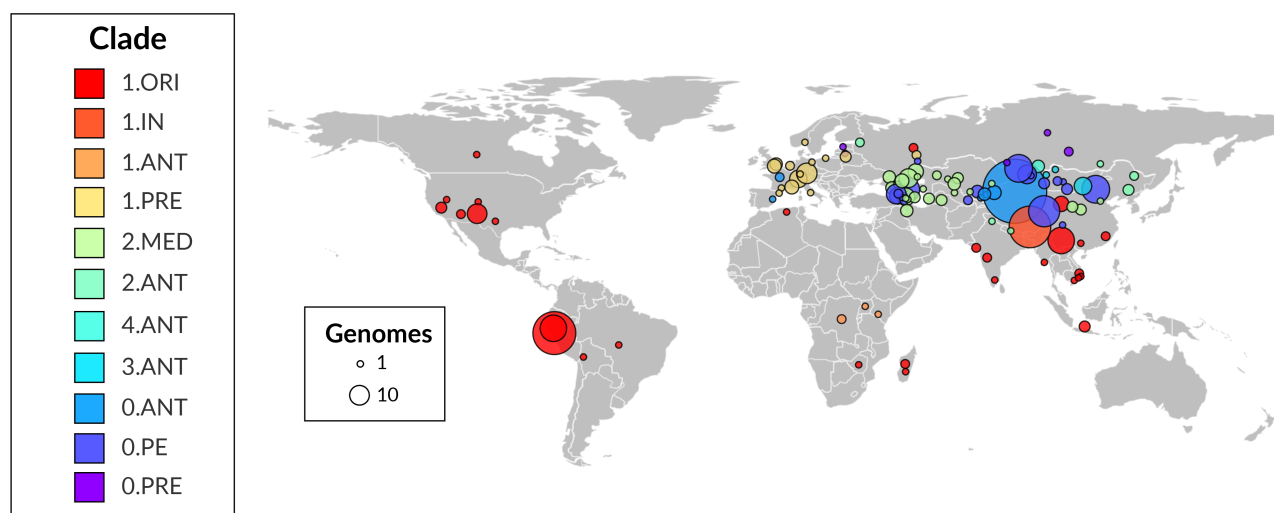
Phylogeography

Geographic location was modeled as a discrete state with transitions following a GTR migration model as implemented in TreeTime [\[23\]](#).

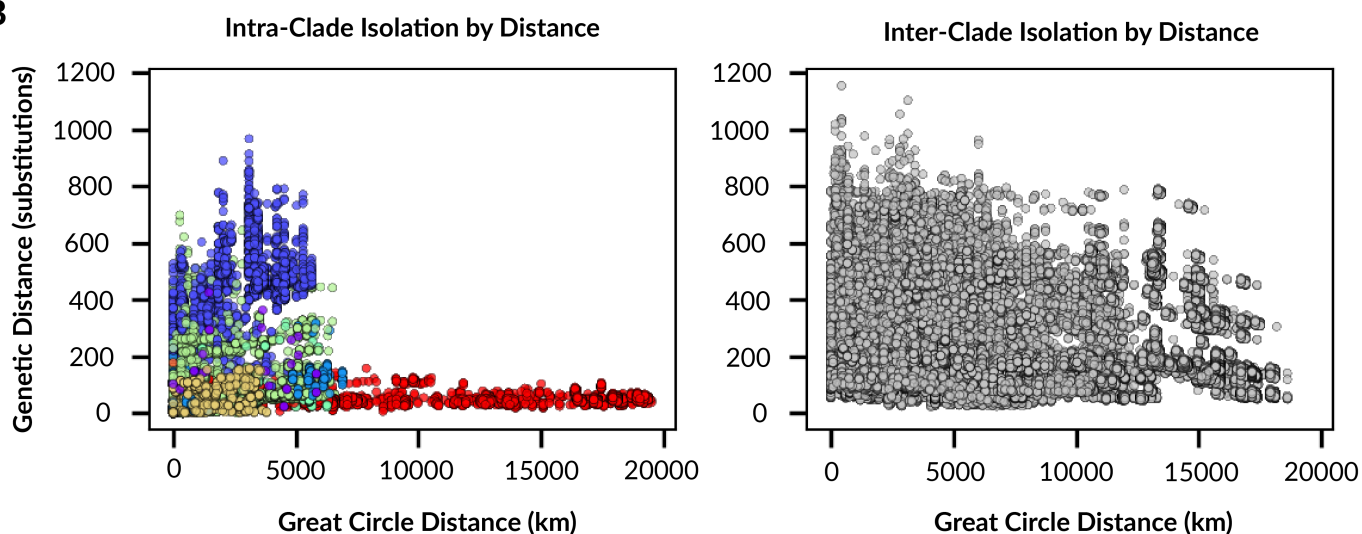
Results

Spatiotemporal Distribution

A



B



C

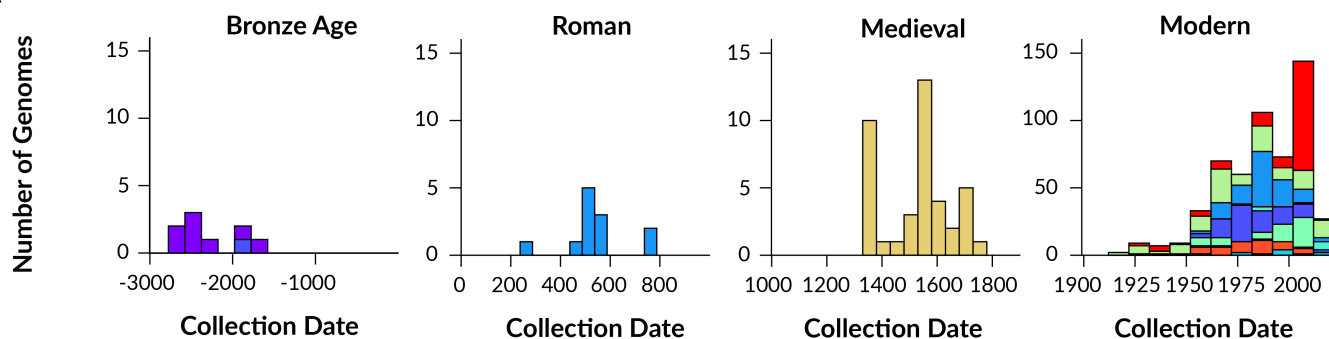


Figure 2: Spatiotemporal distribution of *Y. pestis* genomes. **A:** Geographic distribution, **B:** Isolation by distance as a function of geographic distance and genetic distance, **C:** Temporal distribution.

After careful curation, 600 genomes remained, with 539 (90%) being modern in origin and 61 (10%) being ancient. The spatiotemporal distribution of samples is shown in Figure 2. Three important findings can be drawn from a descriptive summary of the spatiotemporal distribution.

The first finding is that the geographic sampling strategy of *Y. pestis* genomes (Figure 2 .A) does not reflect the known distribution of modern plague [24]. Nor does it adequately characterize the most heavily affected regions of the world, namely Madagascar and the Democratic Republic of the Congo [5]. The over-sampling of East Asia has been previously described by 25 and considerably drives the hypothesis that *Y. pestis* originated in China [18,26]. This once established hypothesis is now in contention, as the most basal strains of *Y. pestis* (Clades 0.PRE and 0.PE) have been isolated from all across Eurasia.

The second observation is that the temporal sampling strategy of genomic data (Figure 2 .C) reflects greater interest in *Y. pestis* as a historical pathogen, rather than a public health threat to modern humans. One example of this is that the Medieval Plague in Western Europe (Clade 1.PRE) has more representative samples than all of the African continent (Clade 1.ANT). Sequencing initiatives are greatly needed that shift the balance away from Eurocentrism and encompass a greater diversity of affected populations.

The final takeaway is a highly complex pattern of geographic clustering or lack thereof (Figure 2 .B). Many regions have been colonized by diverse strains of *Y. pestis*. This diversity can be contemporaneous, such as endemic foci in the Caucasus and Western China (Clade 0.PE). Alternatively, this diversity may occur over multiple centuries through distinct re-introductions and extinctions, as seen in the historical epidemics of Europe (Clade 1.PRE). In these examples, a relatively large amount of genetic diversity appears in a small geographic range. In contrast, regions such as the Americas have been colonized by a single strain of *Y. pestis* (Clade 1.ORI) and shows a relatively small amount of genetic diversity over a tremendously large geographic range.

Taken together, these findings should be taken as a cautionary warning. Given the biases documented here, extrapolating the data runs the risk of reconstructing the *sampling history* of plague researchers, rather than the *natural history* of the disease. This is particularly relevant for analyses that assume an absence of evidence is evidence of absence, such as in phylogeographic reconstruction.

Phylogenetics

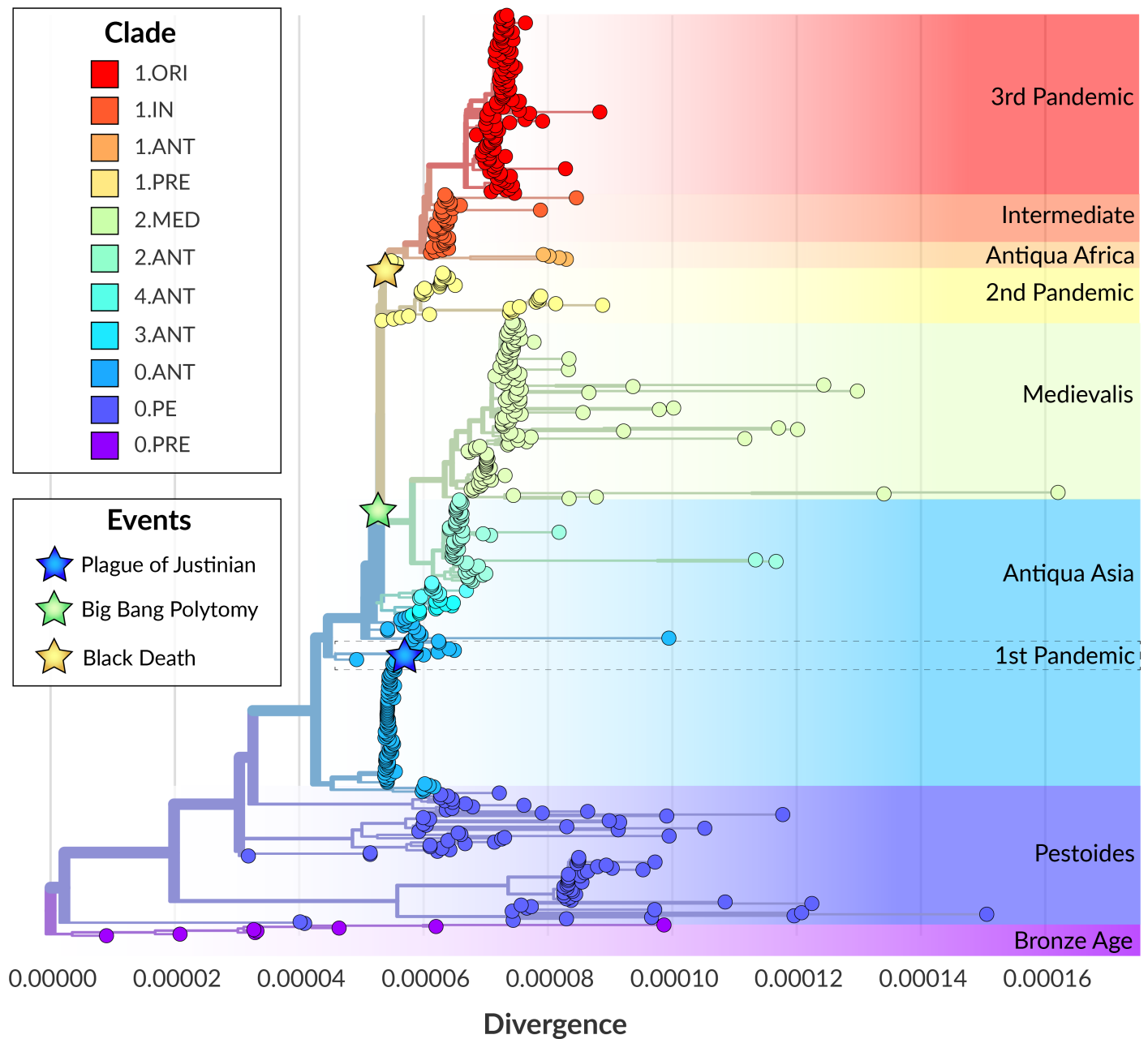


Figure 3: *Y. pestis* maximum-likelihood phylogeny.

What can we learn from the maximum-likelihood phylogeny (Figure 3)?

- **Problems of the Three Pandemic Structure:** There are three historically documented pandemics of plague but...
- **Rate Variation:** *Y. pestis* shows extraordinary rate variation. This can most clearly be seen in samples from the Bronze Age accumulating more substitutions than several modern clades.
- **Ecological Structure:** There is no obvious clustering by host. If there is, its reflects the sampling strategy (ex. Ancient DNA from skeletal remains) rather than the natural history.

Phylodynamics

- *Y. pestis* has extreme rate variation.
- A Root to Tip Regression on collection date confirms this, as the Coefficient of Determination (R^2) is 0.09, revealing a poor fit to a simple linear model (Table 1).
- To some extent, this variation can be explained by examining the clades in isolation (Figure 4).
- Finding an appropriate evolutionary model is key to estimating historic events, like clade emergence (Figure ??).

Table 1: Temporal signal statistics by clade based on a root-to-tip linear regression.

| Branch | Clade | Origin | RTT R^2 | RTT p-value | BETS Bayes Factor |
|--------|--------|-----------------|-----------|-------------|-------------------|
| All | All | Ancient, Modern | 0.09 | 3.81E-14* | |
| 0 | 0.PRE | Ancient | 0.91 | 1.53E-04* | |
| 0 | 0.PE | Modern | 0.01 | 2.25E-01 | |
| 0 | 0.ANT4 | Ancient | 0.66 | 7.84E-04* | |
| 0 | 0.ANT | Modern | -0.01 | 7.35E-01 | |
| 1 | 1.ANT | Modern | 0.45 | 2.03E-01 | |
| 1 | 1.IN | Modern | 0.0 | 3.24E-01 | |
| 1 | 1.ORI | Modern | 0.04 | 1.32E-02* | |
| 1 | 1.PRE | Ancient | 0.76 | 1.68E-13* | |
| 2 | 2.ANT | Modern | 0.05 | 5.96E-02 | |
| 2 | 2.MED | Modern | 0.01 | 1.86E-01 | |
| 3 | 3.ANT | Modern | -0.04 | 4.39E-01 | |
| 4 | 4.ANT | Modern | -0.11 | 8.80E-01 | |

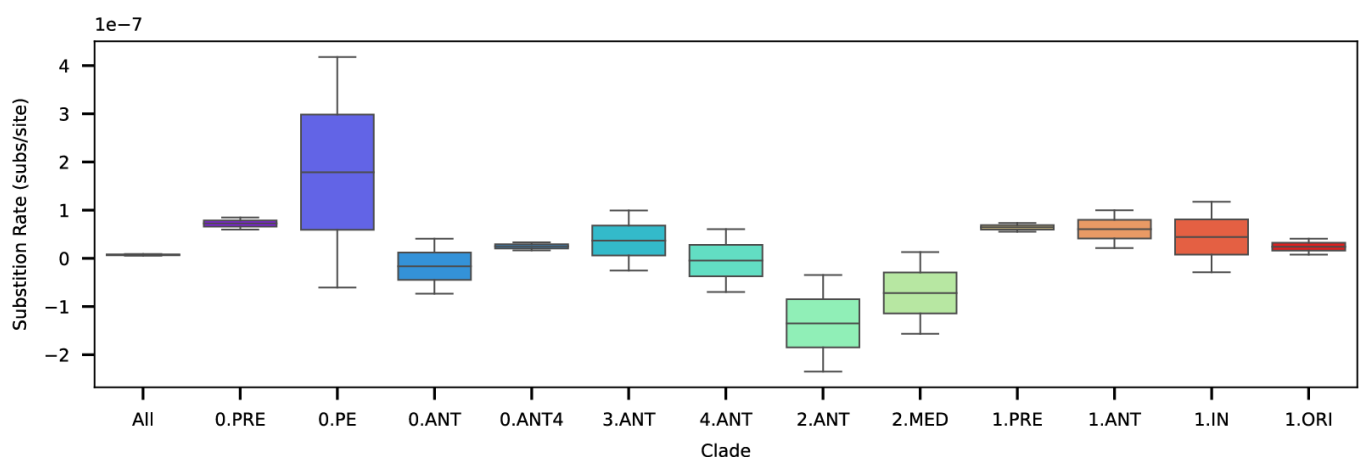


Figure 4: Substitution rate uncertainty by clade based on a root-to-tip linear regression. Highlighted clades are known to be associated with human pandemics.

Relaxing the Clock

- Relaxed clock MCMC runs produce a high Coefficient of Variation indicating a relaxed model is favored over a strict model (Figure 5). However, these runs do not converge, suggesting there is too

much rate variation to confidently estimate key parameters such as the mean Substitution Rate or tMRCA.

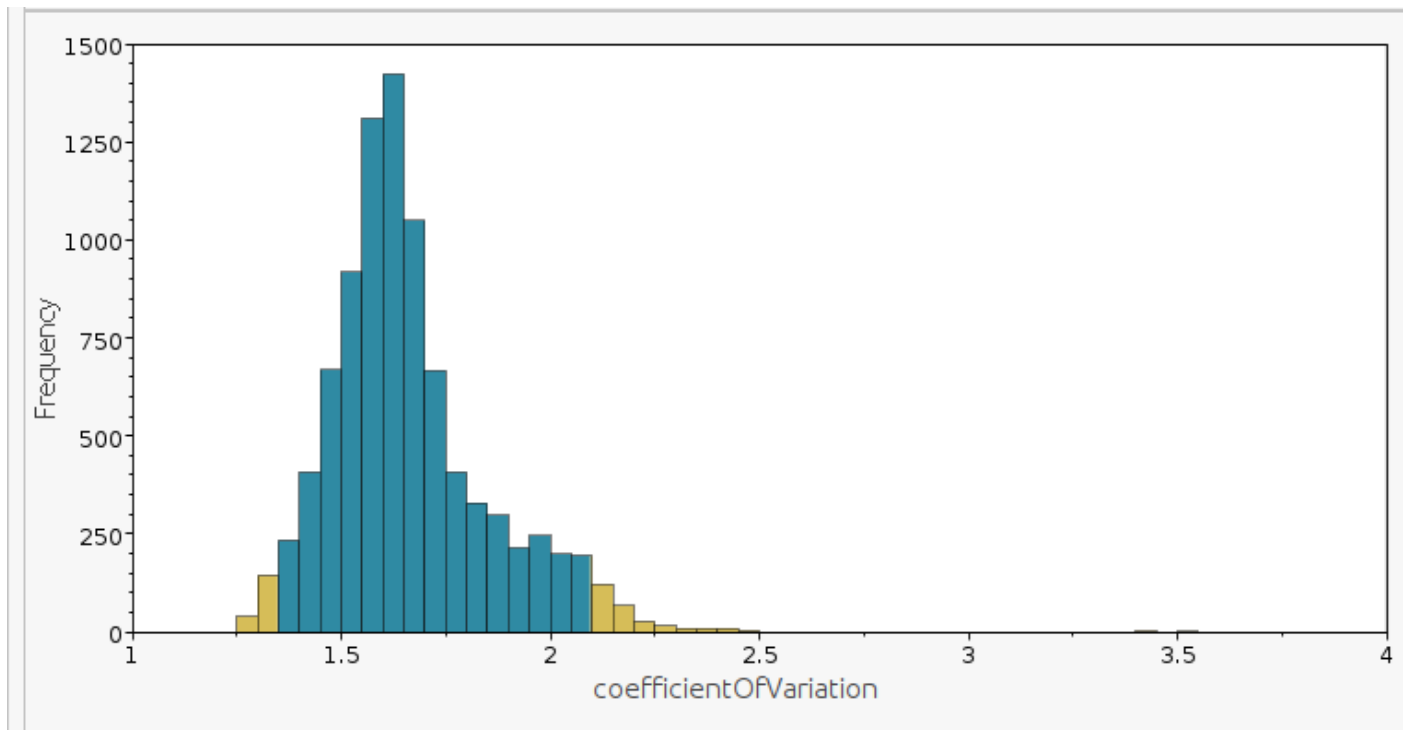


Figure 5: Coefficient of variation.

- A strict clock and relaxed clock have overlapping distributions with similar peaks for the Tree Height (blue: strict, green: relaxed) (Figure 6).

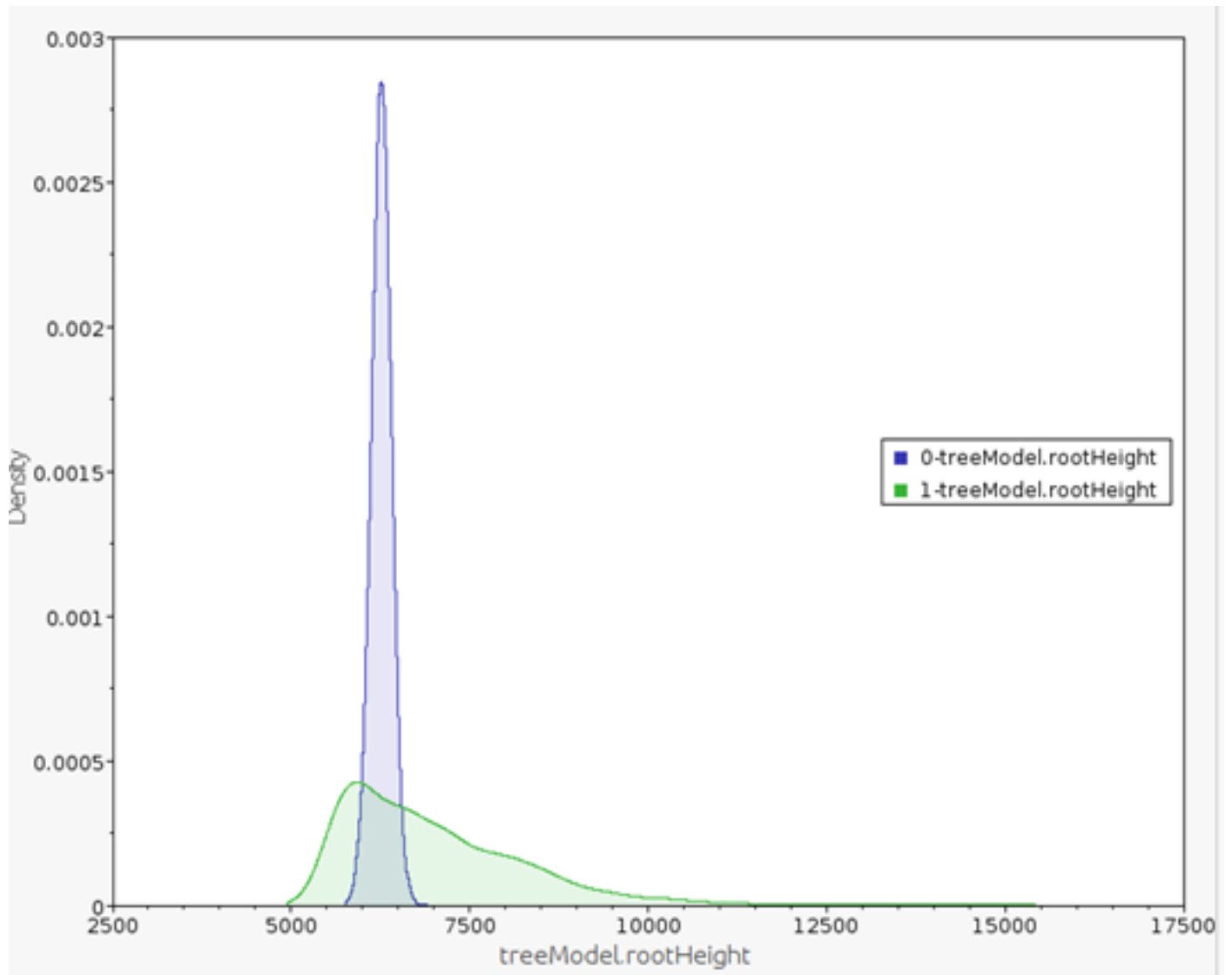


Figure 6: Tree height comparison.

- When estimating a Substitution Rate for all of *Y. pestis*, a [[Clock Model | strict clock]] and relaxed clock produce different estimates (green: strict, orange: relaxed) (Figure 7).

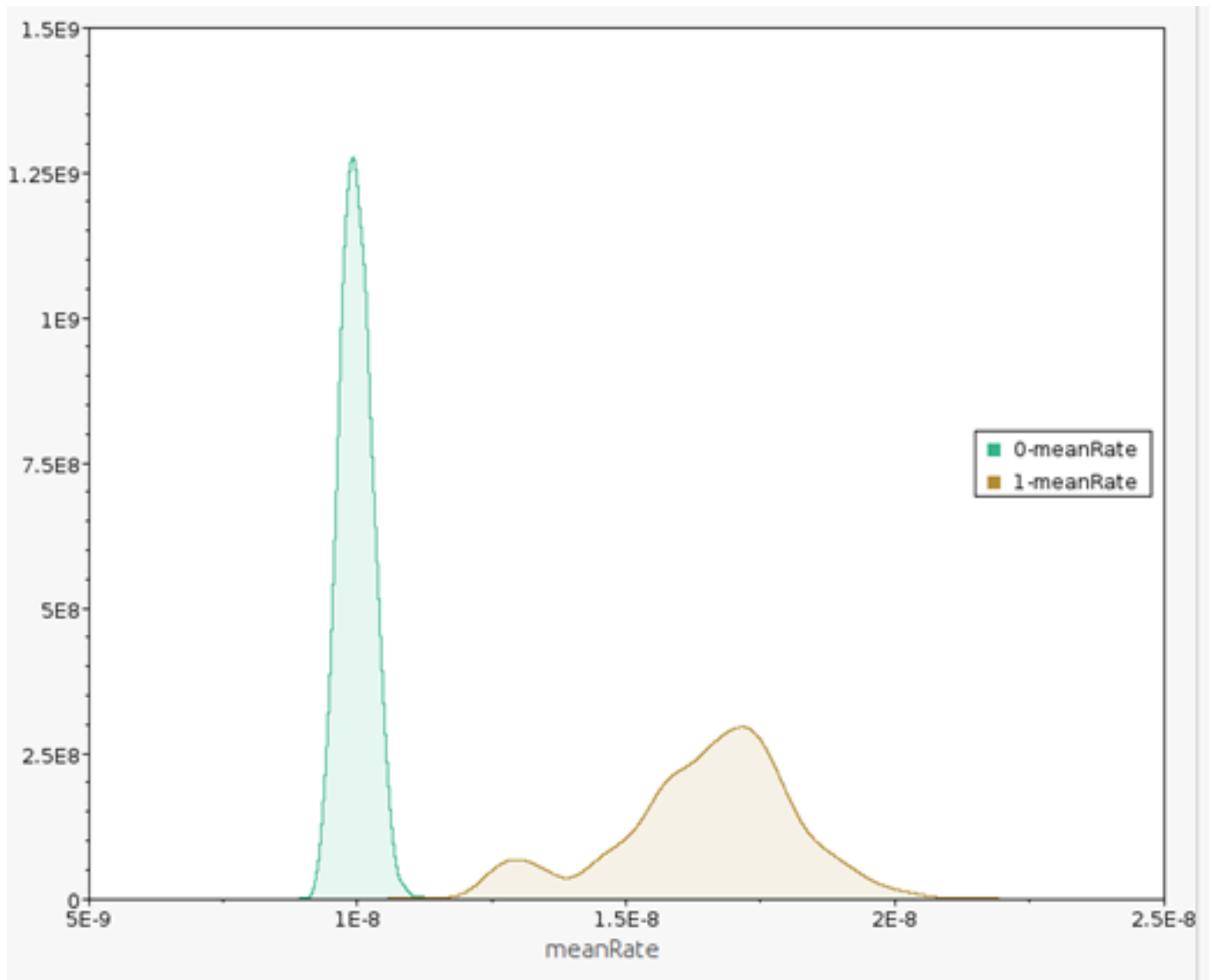


Figure 7: Substitution rate comparison.

- There doesn't appear to be clustering of rates. Branches with high rates are next to those with low rates (Figure [8](#)).

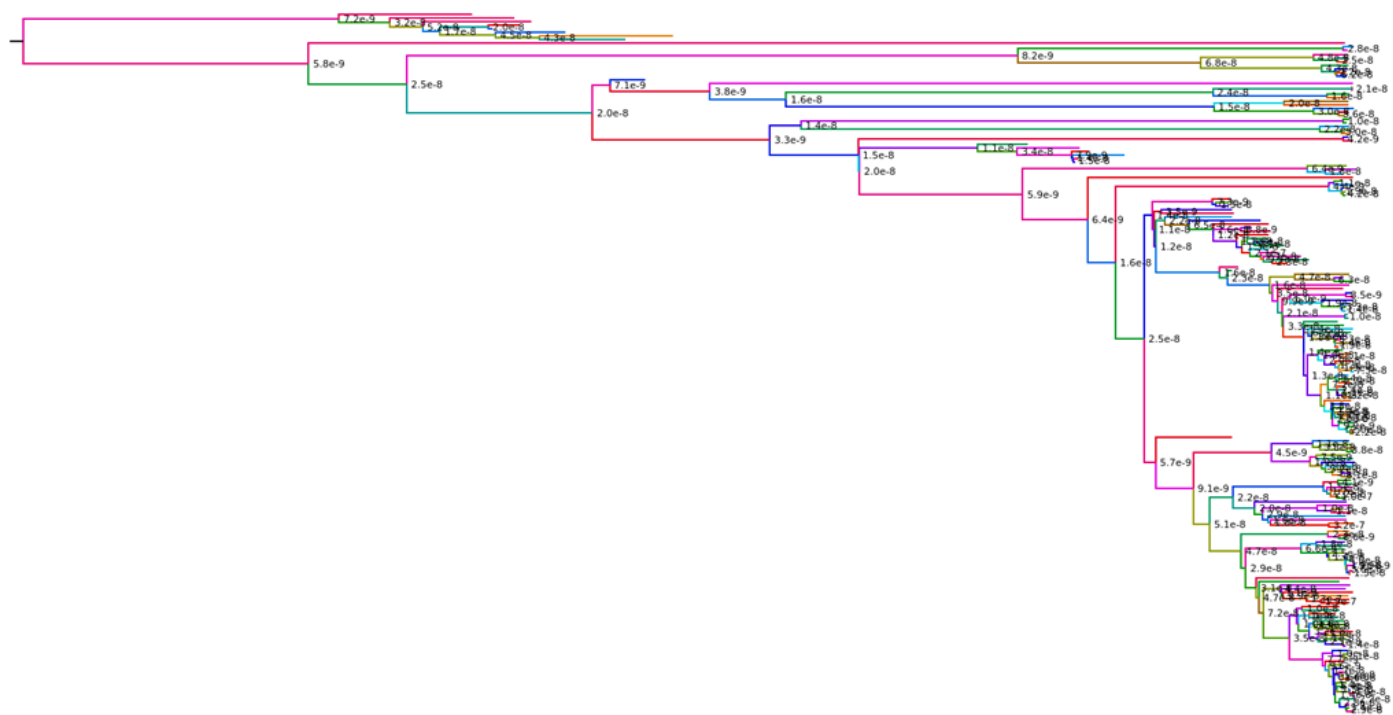


Figure 8: Time tree colored by rate.

Phylogeography

Conclusion

Appendix

References

1. The Stone Age Plague and Its Persistence in Eurasia

Aida Andrades Valtueña, Alissa Mittnik, Felix M. Key, Wolfgang Haak, Raili Allmäe, Andrej Belinskij, Mantas Daubaras, Michal Feldman, Rimantas Jankauskas, Ivor Janković, ... Johannes Krause
Current Biology (2017-12-04)
DOI: [10.1016/j.cub.2017.10.025](https://doi.org/10.1016/j.cub.2017.10.025) · PMID: [29174893](https://pubmed.ncbi.nlm.nih.gov/29174893/)

2. Emergence and spread of basal lineages of *Yersinia pestis* during the Neolithic Decline

Nicolás Rascovan, Karl-Göran Sjögren, Kristian Kristiansen, Rasmus Nielsen, Eske Willerslev, Christelle Desnues, Simon Rasmussen
Cell (2019-01-10) [https://www.cell.com/cell/abstract/S0092-8674\(18\)31464-8](https://www.cell.com/cell/abstract/S0092-8674(18)31464-8)
DOI: [10.1016/j.cell.2018.11.005](https://doi.org/10.1016/j.cell.2018.11.005) · PMID: [30528431](https://pubmed.ncbi.nlm.nih.gov/30528431/)

3. Trade routes and plague transmission in pre-industrial Europe

Ricci P. H. Yue, Harry F. Lee, Connor Y. H. Wu
Scientific Reports (2017-10-11) <https://www.ncbi.nlm.nih.gov/pmc/articles/PMC5636801/>
DOI: [10.1038/s41598-017-13481-2](https://doi.org/10.1038/s41598-017-13481-2) · PMID: [29021541](https://pubmed.ncbi.nlm.nih.gov/29021541/) · PMCID: [PMC5636801](https://pubmed.ncbi.nlm.nih.gov/PMC5636801/)

4. *Yersinia pestis*-etiologic agent of plague

R. D. Perry, J. D. Fetherston
Clinical Microbiology Reviews (1997-01)
PMID: [8993858](https://pubmed.ncbi.nlm.nih.gov/8993858/) · PMCID: [PMC172914](https://pubmed.ncbi.nlm.nih.gov/PMC172914/)

5. Plague

World Health Organization
(2017-10-31) <https://www.who.int/news-room/fact-sheets/detail/plague>

6. The Black Death, 1346-1353: The Complete History

O. J. Benedictow
Boydell Press (2004)
ISBN: [0-85115-943-5](https://www.isbn-international.org/product/0-85115-943-5)

7. Plague around the world in 2019

Eric Bertherat
Weekly Epidemiological Record (2019-06-21) <https://apps.who.int/iris/bitstream/handle/10665/325481/WER9425-en-fr.pdf>

8. Recent trends in plague ecology

K Gage, M Kosoy
(2006) http://reviverestore.org/wp-content/uploads/2015/02/Gage-and-Kosoy_USGS-Blk-footed-ferret-symp_2006-copy.pdf

9. *Yersinia pestis*, the cause of plague, is a recently emerged clone of *Yersinia pseudotuberculosis*

M. Achtman, K. Zurth, G. Morelli, G. Torrea, A. Guiyoule, E. Carniel
Proceedings of the National Academy of Sciences of the United States of America (1999-11-23)
DOI: [10.1073/pnas.96.24.14043](https://doi.org/10.1073/pnas.96.24.14043) · PMID: [10570195](https://pubmed.ncbi.nlm.nih.gov/10570195/) · PMCID: [PMC24187](https://pubmed.ncbi.nlm.nih.gov/PMC24187/)

10. **Insights into the evolution of *Yersinia pestis* through whole-genome comparison with *Yersinia pseudotuberculosis***
P. S. G. Chain, E. Carniel, F. W. Larimer, J. Lamerdin, P. O. Stoutland, W. M. Regala, A. M. Georgescu, L. M. Vergez, M. L. Land, V. L. Motin, ... E. Garcia
Proceedings of the National Academy of Sciences (2004-09-21) <http://www.pnas.org/cgi/doi/10.1073/pnas.0404012101>
DOI: [10.1073/pnas.0404012101](https://doi.org/10.1073/pnas.0404012101)
11. **NCBImeta**
Katherine Eaton
NCBImeta (2019) <https://github.com/ktmeaton/NCBImeta>
12. **GeoPy: A Python client for several popular geocoding web services.**
Kostya Esmukov
(2020-12) <https://github.com/geopy/geopy>
13. **Nominatim: A tool to search OpenStreetMap data.**
Sarah Hoffman
(2020-12) <https://github.com/osm-search/Nominatim>
14. **Planet dump retrieved from <https://planet.osm.org>**
OpenStreetMap Contributors
(2017) <https://www.openstreetmap.org>
15. **Snippy: Rapid haploid variant calling and core genome alignment.**
Torsten Seemann
(2020-03-08) <https://github.com/tseemann/snippy>
16. **ncbi/sra-tools**
NCBI - National Center for Biotechnology Information/NLM/NIH
(2021-05-18) <https://github.com/ncbi/sra-tools>
17. **Reproducible, portable, and efficient ancient genome reconstruction with nf-core/eager**
James A. Fellows Yates, Thisseas C. Lamnidis, Maxime Borry, Aida Andrades Valtueña, Zandra Fagernäs, Stephen Clayton, Maxime U. Garcia, Judith Neukamm, Alexander Peltzer
PeerJ (2021-03-16) <https://peerj.com/articles/10947>
DOI: [10.7717/peerj.10947](https://doi.org/10.7717/peerj.10947)
18. **Historical variations in mutation rate in an epidemic pathogen, *Yersinia pestis***
Y. Cui, C. Yu, Y. Yan, D. Li, Y. Li, T. Jombart, L. A. Weinert, Z. Wang, Z. Guo, L. Xu, ... R. Yang
Proceedings of the National Academy of Sciences (2013-01-08) <http://www.pnas.org/cgi/doi/10.1073/pnas.1205750110>
DOI: [10.1073/pnas.1205750110](https://doi.org/10.1073/pnas.1205750110)
19. **ModelFinder: fast model selection for accurate phylogenetic estimates**
Subha Kalyaanamoorthy, Bui Quang Minh, Thomas K. F. Wong, Arndt von Haeseler, Lars S. Jermini
Nature Methods (2017-06) <http://www.nature.com/articles/nmeth.4285>
DOI: [10.1038/nmeth.4285](https://doi.org/10.1038/nmeth.4285)

20. **IQ-TREE 2: New Models and Efficient Methods for Phylogenetic Inference in the Genomic Era**
Bui Quang Minh, Heiko A. Schmidt, Olga Chernomor, Dominik Schrempf, Michael D. Woodhams, Arndt von Haeseler, Robert Lanfear
Molecular Biology and Evolution (2020-05-01) <https://academic.oup.com/mbe/article/37/5/1530/5721363>
DOI: [10.1093/molbev/msaa015](https://doi.org/10.1093/molbev/msaa015)
21. **UFBoot2: Improving the Ultrafast Bootstrap Approximation**
Diep Thi Hoang, Olga Chernomor, Arndt von Haeseler, Bui Quang Minh, Le Sy Vinh
Molecular Biology and Evolution (2018-02-01) <https://academic.oup.com/mbe/article/35/2/518/4565479>
DOI: [10.1093/molbev/msx281](https://doi.org/10.1093/molbev/msx281)
22. **Fast Dating Using Least-Squares Criteria and Algorithms**
Thu-Hien To, Matthieu Jung, Samantha Lycett, Olivier Gascuel
Systematic Biology (2016-01) <https://academic.oup.com/sysbio/article-lookup/doi/10.1093/sysbio/syv068>
DOI: [10.1093/sysbio/syv068](https://doi.org/10.1093/sysbio/syv068)
23. **TreeTime: Maximum-likelihood phylodynamic analysis**
Pavel Sagulenko, Vadim Puller, Richard A Neher
Virus Evolution (2018-01-08) <https://www.ncbi.nlm.nih.gov/pmc/articles/PMC5758920/>
DOI: [10.1093/ve/vex042](https://doi.org/10.1093/ve/vex042) · PMID: [29340210](https://pubmed.ncbi.nlm.nih.gov/29340210/) · PMCID: [PMC5758920](https://pubmed.ncbi.nlm.nih.gov/PMC5758920/)
24. **Historical and genomic data reveal the influencing factors on global transmission velocity of plague during the Third Pandemic**
Lei Xu, Leif C. Stige, Herwig Leirs, Simon Neerinx, Kenneth L. Gage, Ruifu Yang, Qiyong Liu, Barbara Bramanti, Katharine R. Dean, Hui Tang, ... Zhibin Zhang
Proceedings of the National Academy of Sciences (2019-06-11) <https://www.pnas.org/content/116/24/11833>
DOI: [10.1073/pnas.1901366116](https://doi.org/10.1073/pnas.1901366116) · PMID: [31138696](https://pubmed.ncbi.nlm.nih.gov/31138696/)
25. **Historical *Y. pestis* Genomes Reveal the European Black Death as the Source of Ancient and Modern Plague Pandemics**
Maria A. Spyrou, Rezeda I. Tukhbatova, Michal Feldman, Joanna Drath, Sacha Kacki, Julia Beltrán de Heredia, Susanne Arnold, Airat G. Sitdikov, Dominique Castex, Joachim Wahl, ... Johannes Krause
Cell Host & Microbe (2016-06) <http://linkinghub.elsevier.com/retrieve/pii/S1931312816302086>
DOI: [10.1016/j.chom.2016.05.012](https://doi.org/10.1016/j.chom.2016.05.012)
26. ***Yersinia pestis* genome sequencing identifies patterns of global phylogenetic diversity**
Giovanna Morelli, Yajun Song, Camila J. Mazzoni, Mark Eppinger, Philippe Roumagnac, David M. Wagner, Mirjam Feldkamp, Barica Kusecek, Amy J. Vogler, Yanjun Li, ... Mark Achtman
Nature Genetics (2010-12)
DOI: [10.1038/ng.705](https://doi.org/10.1038/ng.705) · PMID: [21037571](https://pubmed.ncbi.nlm.nih.gov/21037571/) · PMCID: [PMC2999892](https://pubmed.ncbi.nlm.nih.gov/PMC2999892/)